

# Selecting and ranking interesting pairs of cyclic temporal granularities

## Contents

<b>1</b>	<b>Introduction</b>	<b>1</b>
<b>2</b>	<b>The proposed distance measure</b>	<b>5</b>
2.1	Idea . . . . .	5
2.2	Characterising distributions . . . . .	5
2.3	Distance between distributions . . . . .	7
2.4	Definition of the proposed distance measure . . . . .	7
2.5	Normalisation . . . . .	7
2.6	Simulation study . . . . .	8
2.7	Properties . . . . .	10
<b>3</b>	<b>Choosing harmonies with significant wpd</b>	<b>10</b>
<b>4</b>	<b>Applications</b>	<b>10</b>
4.1	Smart meter data of Australia . . . . .	10
4.2	T20 cricket data of Indian Premiere League . . . . .	10
<b>5</b>	<b>Discussion points and future work</b>	<b>11</b>
<b>6</b>	<b>Appendix</b>	<b>11</b>
6.1	Null distribution . . . . .	11
6.2	Power . . . . .	13
6.3	Confidence interval . . . . .	13

## 1 Introduction

Exploratory data analysis, as coined by John W. Tukey (Tukey 1965) involves many iterations of finding structures and patterns that allows the data to be informative. With temporal data available at finer scales, exploring periodicity and their relationships can become overwhelming with so many possible cyclic temporal granularities (Gupta et al. 2020) to explore.

Take the example of the calendar display of electricity smart meter data (1) used in Wang, Cook, and Hyn-dman (2020) for four households in Melbourne, Australia. The authors show how hour-of-the-day interact

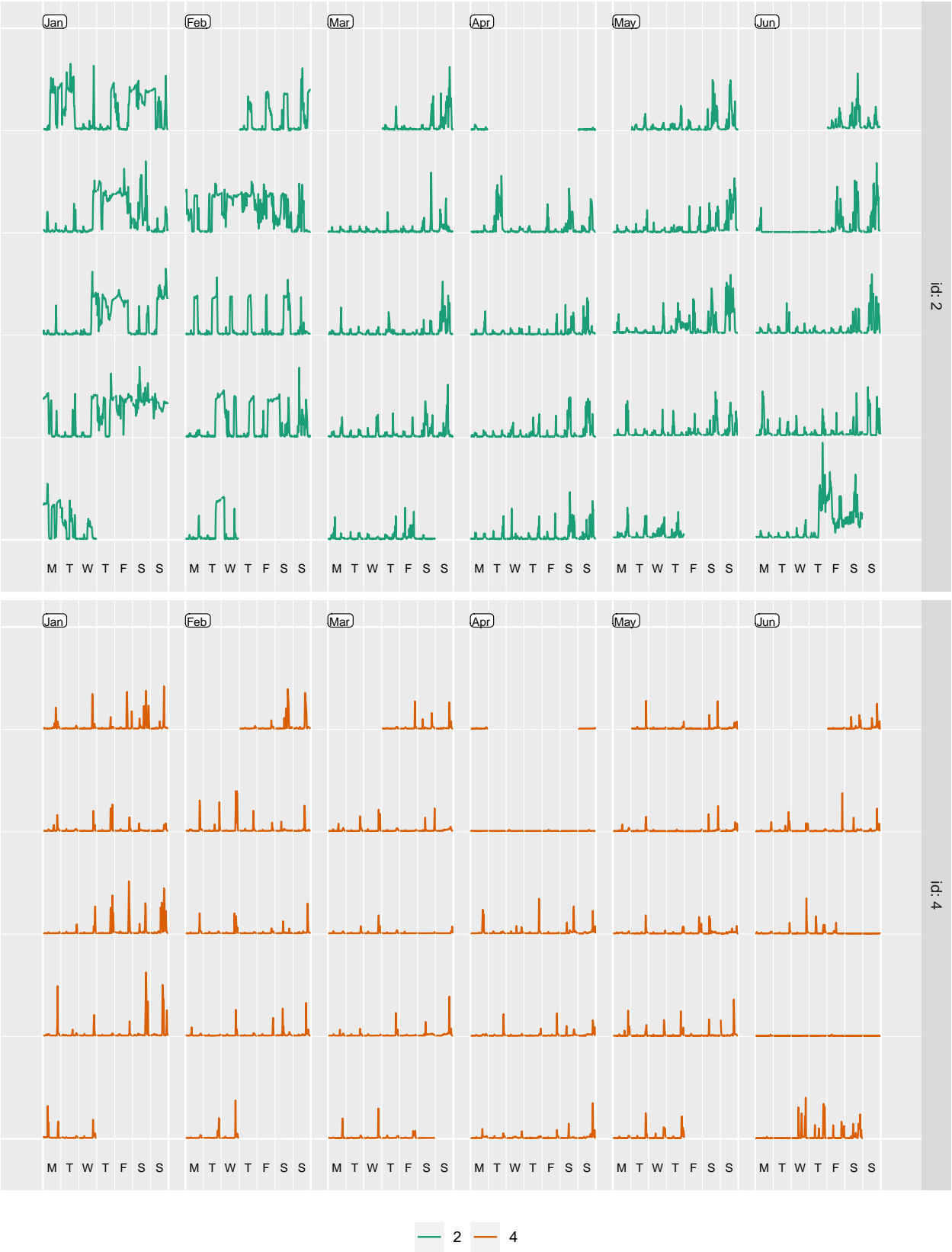


Figure 1: Calendar display.

with weekday and weekends and then move on to use calendar display to show daily schedules. The calendar display has several components in it, which helps us look at energy consumption across hour-of-the-day, day-of-the-week, week-of-the-month, and month-of-the-year at once. Some interaction of these cyclic granularities could also be interpreted from this display. This is a great start to have an overview of the energy consumption. However, if one wants to understand the periodicities in energy behavior and how the periodicities interact in greater details, it is not easy to comprehend the interactions of some periodicities' from this display, due to the combination of linear and cyclic representation of time. For example, this display might not be the best to understand how hour-of-the-day varies and month-of-year varies across week-of-the-month. Further, it is not clear what all interactions of cyclic granularities should be read from this display as there could be many combinations that one can look at. Moreover, calendar effects are not restricted to conventional day-of-week or month-of-year deconstructions (Gupta et al. (2020)) and could include other cyclic granularities like hour-of-week or day-of-fortnight, which could potentially become useful depending on the context.

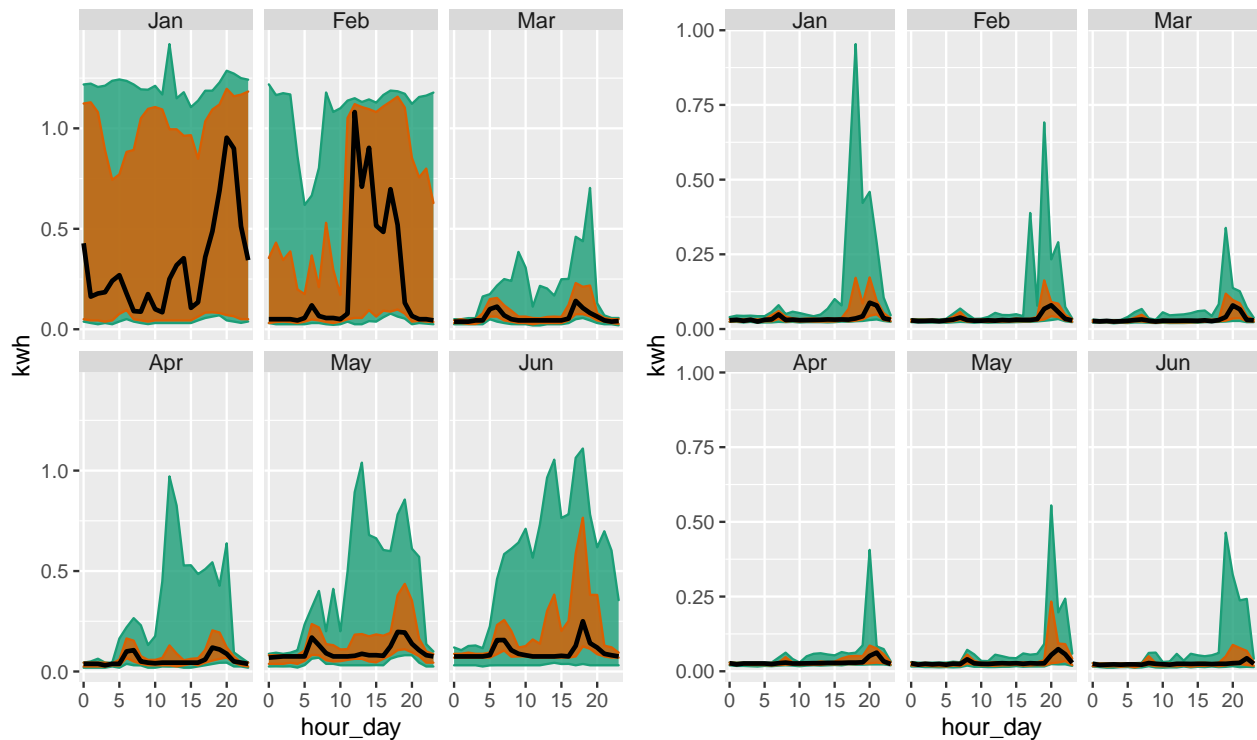


Figure 2: something

Moreover, there might be specific interactions that are interesting and others that are not and that too will vary with different households. For example, area distribution quantiles are plotted for household 2 and 4 in Figure 2a and b respectively. For the first household, the 75th and 90th percentile for Jan, Feb and July are very close, implying that energy usage for these months are generally on a much higher side due to the usage of air conditioners (in Jan and Feb) and heaters (in July). The energy consumption for household 2 is also higher relative to its own consumption for Jan, Feb and March but the 75th and 90th percentile are apart implying that contrary to the first household, the second household resorts to air conditioners and heaters much less regularly than the first one. Moreover, the 75th percentile distribution is not bimodal across hours of the day for the first household in those months, but the distribution looks similar for all months for the second household. Difference in the energy consumption seem to be varying both across month-of-year (facets) and hour-of-day (x-axis). And thus, both the cyclic granularities would deem important while studying the periodicities in the first household. However, it seems like energy consumption across hours of the day are not that different across different months for the second household. Differences seem to be more prominent across month-of-year (facets) than hour-of-day (x-axis). Again, look at ?? c and d, where energy

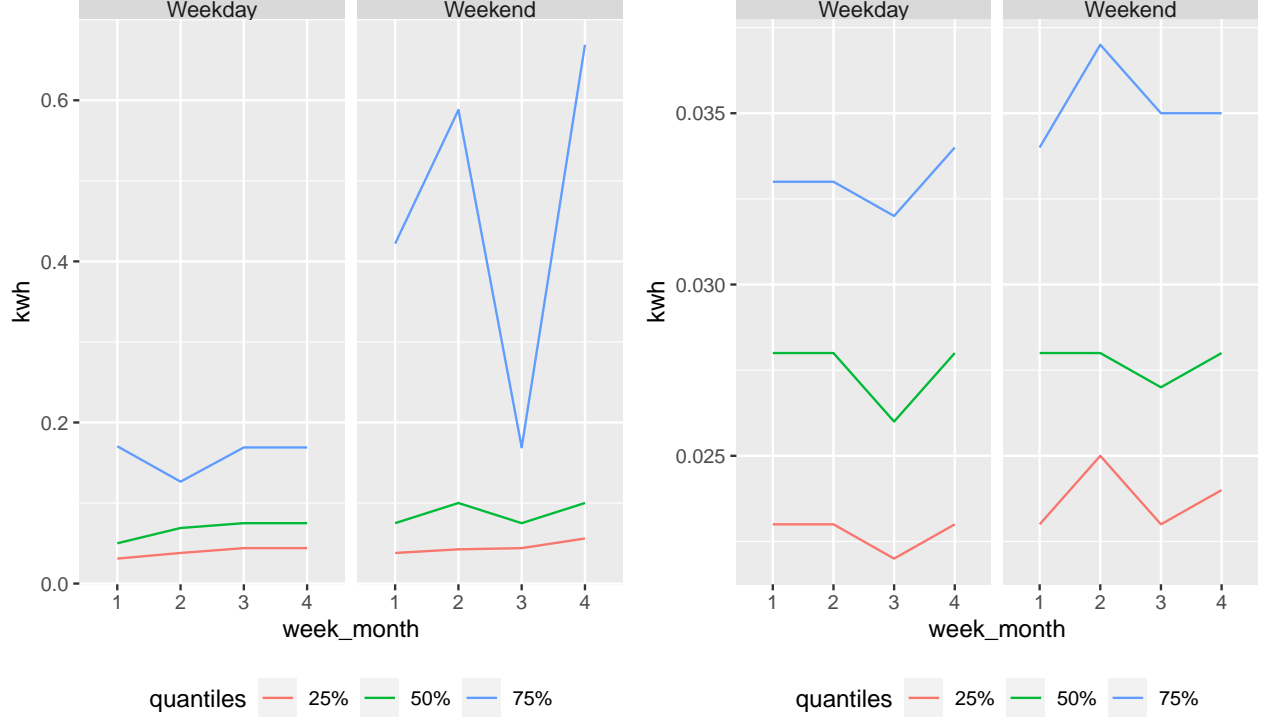


Figure 3: something2

consumption for these two households are plotted against (weekend/weekday, week-of-month). Here, for both households, the pattern of energy consumption vary across different weeks of the month irrespective of the fact it is a weekday or weekend. In that respect, the harmony pair (month-of-year, hour-of-day) seems to be more informative than (weekend/weekday, week-of-month) for the first household. It could be immensely useful to make the transition from all possible ways to only ways that could potentially be informative given a household.

The paper Gupta et al. (2020) describes how we can compute all possible combinations of cyclic time granularities. If we have  $n$  periodic linear granularities in the hierarchy table, then  $n(n-1)/2$  circular or quasi-circular cyclic granularities could be constructed. Let  $N_C$  be the total number of contextual circular, quasi-circular and aperiodic cyclic granularities that can originate from the underlying periodic and aperiodic linear granularities. The mapping of the graphical elements chosen in the paper implies that, for a numeric response variable, the graphics display distributions across combinations of cyclic granularities, one placed at x-axis and the other on the facet. That essentially implies there are  $N_C P_2$  possible pairwise plots exhaustively, where each plot would display a pair of cyclic granularities. This is large and overwhelming for human consumption.

This is similar to Scagnostics (Scatterplot Diagnostics) by Tukey and Tukey (1988), which is used to discern meaningful patterns in large collections of scatterplots. Given a set of  $v$  variables, there are  $v(v-1)/2$  pairs of variables, and thus the same number of possible pairwise scatterplots. Therefore for even small  $v$ , the number of scatterplots can be large, and scatterplot matrices (SPLOMs) could easily run out of pixels when presenting high-dimensional data. Dang and Wilkinson (2014) and Wilkinson, Anand, and Grossman (2005) provides potential solutions to this, where few characterizations help us to locate anomalies for defining several measures aimed to detect anomalies in density, shape, trend, and other features in the 2D point scatters.

The paper (Gupta et al. (2020)) narrows down the search from  $N_C P_2$  plots by identifying pairs of granularities that can be meaningfully examined together (a “harmony”), or when they cannot (a “clash”). However, even after excluding clashes, the list of harmonies left could be enormous for exhaustive exploration. Hence, there

is a need to reduce the search even further by including only those harmonies which are informative enough. Also, ranking the remaining harmony pairs based on how well they capture the variation in the measured variable could be potentially useful.

In this paper, we aim to build a new measure to follow through these two main objectives:

- To choose harmonies for which distributions of categories are significantly different
- To rank the selected harmonies from highest to lowest variation in the distribution of their categories.

## 2 The proposed distance measure

We are interested in assessing structure in probability distributions of the measured variable across bivariate cyclic granularities. We propose a measure called Weighted Maximum Pairwise Distances (wpd) to evaluate structure in such a design.

### 2.1 Idea

The principle employed for building a new metric is explained through a simple example explained in Figure 4. Each of these figures have the same panel design with 2 x-axis categories and 4 facet levels. Figure 4a has all x categories drawn from  $N(5, 10)$  distribution for each facet. It is not an interesting display particularly, as distributions do not vary across x-axis or facet categories. Figure 4b has x categories drawn from the same distribution within a facet and different for different facet categories. Figure 4b exhibits an exact opposite situation where distribution between the x-axis categories within each facet is different but they are same across facets. Figure 4d takes a step further by varying the distribution across both facet and x-axis categories. If we are asked to rank the displays in order of importance from minimum to maximum, we might order it as a, b, c and then d. It might be argued that it is not clear if b should precede or succeed c. Gestalt theory suggests that when items are placed in close proximity, people assume that they are in the same group because they are close to one another and apart from other groups. Hence, displays that capture more variation within different categories in the same group would be important to bring out different patterns of the data. With this principle, display b could be considered less informative as compared to display c.

With reference to the graphical design in ??, therefore the idea would be to rate a harmony pair higher if the variation between different levels of the x-axis variable is higher on an average across all levels of the facet variables. Thus the metric could be obtained by computing maximum pairwise distances between distributions of the continuous random variable across x-axis categories for all facets and then taking the median of those maximum pairwise distances across facets. This would help capture the average maximum difference in distribution of the measurement variable explained by the two cyclic granularities together. We call this metric wpd which stands for Median Maximum Pairwise Distances. In the next section we shall see how we go about computing this measure.

### 2.2 Characterising distributions

Each of the data subsets in the data structure have multiple observations and may vary widely across different subsets due to the structure of the calendar, missing observations or uneven locations of events in the time domain. The set of observations corresponding to each combination is assumed to be a sample from an unknown probability density function. While the whole population of observations has certain characteristics, we can typically never measure all of them. Often shape, central tendency, and variability are the common characteristics used to describe the distribution. Another way to describe the probability distribution is through quantiles. (Define quantiles here) Sample quantiles could be thought to estimate the population quantiles. But there are a large number of different definitions used for sample quantiles. The median-unbiased estimator is recommended (Rob's paper) because of its desirable properties of a quantile estimator and can be defined independently of the underlying distribution.



Figure 4: A graphical display with two categories mapped to x-axis and 4 categories mapped to facets with the distribution of a continuous random variable plotted on the y-axis. Display a is not interesting as the distribution of the continuous rv does not depend across x-axis or facet categories. Display b and c are more interesting than a since there is a change in distribution either across facets(b) or x-axis(a). Display d is most interesting as distribution of the rv changes across both facet and x-axis variable.

## 2.3 Distance between distributions

The most common divergence measure between distributions is the Kullback-Leibler (KL) divergence (Kullback and Leibler 1951) introduced by Solomon Kullback and Richard Leibler in 1951. The KL divergence, denoted  $D(p(x), q(x))$  is a non-symmetric measure of the difference between two probability distributions  $p(x)$  and  $q(x)$  and is interpreted as the amount of information lost when  $q(x)$  is used to approximate  $p(x)$ . Although the KL divergence measures the “distance” between two distributions, it is not a distance measure since it is not symmetric and does not satisfy the triangle inequality. The Jensen-Shannon divergence (Menéndez et al. 1997) based on the Kullback-Leibler divergence is symmetric and it always has a finite value. The square root of the Jensen-Shannon divergence is a metric, often referred to as Jensen-Shannon distance. Other common measures of distance are Hellinger distance, total variation distance and Fisher information metric.

In the context of this paper, the pairwise distances between the distributions of the measured variable are computed through Jensen-Shannon distance (JSD) which is based on Kullback-Leibler divergence and is defined by,

$$JSD(P||Q) = \frac{1}{2}D(P||M) + \frac{1}{2}D(Q||M)$$

where  $M = \frac{P+Q}{2}$  and  $D(P||Q) := \int_{-\infty}^{\infty} p(x)f(\frac{p(x)}{q(x)})$  is the KL divergence between distributions  $p(x)$  and  $q(x)$ . Probability distributions are estimated through quantiles instead of kernel density so that there is minimal dependency on selecting kernel or bandwidth.

## 2.4 Definition of the proposed distance measure

Consider two cyclic granularities  $A$  and  $B$ , such that  $A = \{a_j : j = 1, 2, \dots, J\}$  and  $B = \{b_k : k = 1, 2, \dots, K\}$  with  $A$  placed across x-axis and  $B$  across facets. Let the pairwise distances between pairs  $(a_j b_k, a_{j'} b_{k'})$  be denoted as  $d_{(jk),(j'k')} = JSD(a_j b_k, a_{j'} b_{k'})$ . Pairwise distances could be within-facets or between-facets. Figure 5 illustrates how the within-facet or between-facet distances are defined. Pairwise distances are within-facets ( $d_w$ ) when  $b_k = b_{k'}$ , that is, between pairs of the form  $(a_j b_k, a_{j'} b_k)$  as shown in panel (3) of Figure 5. If categories are ordered (like all temporal cyclic granularities), then only distances between pairs where  $a_{j'} = (a_{j+1})$  are considered (panel (4)). Pairwise distances are between-facets ( $d_b$ ) when they are considered between pairs of the form  $(a_j b_k, a_j b_{k'})$ .

From Section 2.1, the idea is to put more weights on within-facet distances than between-facet distances. Hence, for a suitable tuning parameter  $\lambda > 1$ , the pairwise distances  $d_{(jk),(j'k')}$  are transformed based on the distance type as follows:

$$d_{(j,k),(j',k')}^* = \begin{cases} \lambda d_{(jk),(j'k')}, & \text{if } d = d_w \\ (1 - \lambda) d_{(jk),(j'k')}, & \text{if } d = d_b \end{cases} \quad (1)$$

The maximum weighted pairwise distances are defined as:

$$WPD = \max_{j,j',k,k'} (d_{(jk),(j'k')}^*) \forall j, j' \in \{1, 2, \dots, J\}, k, k' \in \{1, 2, \dots, K\}$$

## 2.5 Normalisation

The distribution of wpd is different for different levels of facets and x-axis levels. This is because the statistic maximum which is used to define wpd is affected by the number of categories. The measure would have higher values if  $C_i$  or  $C_j$  has higher levels. However, we would ideally want a higher value of the measure

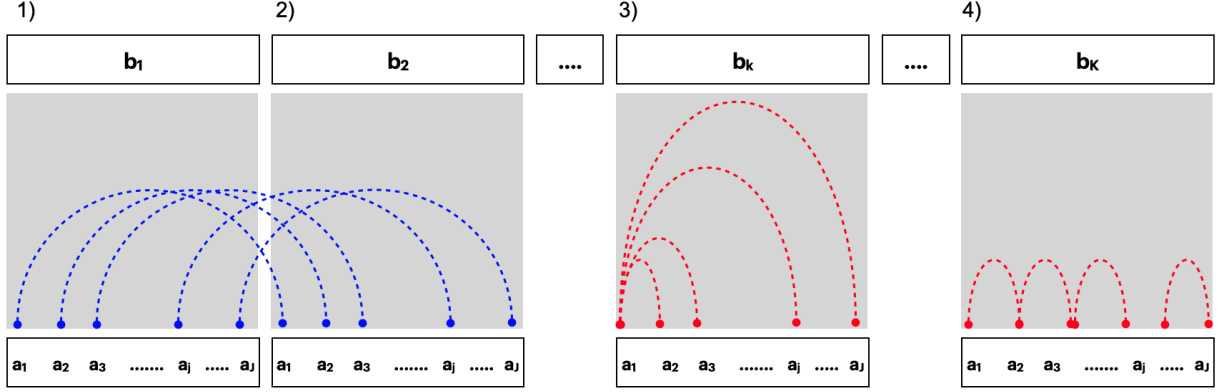


Figure 5: Within and between-facet distances shown for two cyclic granularities A and B, where A is mapped to x-axis and B is mapped to facets. The dotted lines represent the distances between different categories. Panel 1) and 2) show the between-facet distances. Panel 3) and 4) are used to illustrate within-facet distances when categories are un-ordered or ordered respectively. When categories are ordered, distances should only be considered for consecutive x-axis categories. Between-facet distances are distances between different facet levels for the same x-axis category, for example, distances between  $(a_1, b_1)$  and  $(a_1, b_2)$  or  $(a_1, b_1)$  and  $(a_1, b_3)$ .

only if there is significant difference between distributions across facet or x-axis categories, and not because the number of categories are higher. Therefore, in order to compare wpd across different combinations of facet and x-axis levels, we need to eliminate the impact of different levels of the facets and x-axis first and get a normalized measure. Henceforth we call the measure discussed as  $wpd_{raw}$  and the normalised measure as  $wpd_{norm}$ . The measure  $wpd_{norm}$  could potentially lead to comparison of the measure across different panels and also identifying only the interesting panels from a dataset.

## 2.6 Simulation study

Most of the behavior of the measure wpd was studied via simulation. The simulations explore how wpd performs under various designs and parameters and its limitations. To study the behavior of wpd, simulations were carried out for four different designs and the following factors that could potentially have an impact on the values of wpd:

- $nx$  (number of levels of x-axis)
- $n_{facet}$  (number of levels of facets)
- $\lambda$  (tuning parameter)
- $\omega$  (increment in each panel design)
- $dist$  (normal/non-normal distributions with different location and scale)
- $n$  (sample size for each combination of categories)
- $nsim$  (number of simulations)
- $nperm$  (number of permutations of data)
- *designs*
  - $D_{null}$  (No difference in distribution)
  - $D_{var_f}$  (Difference in distribution only across facets)
  - $D_{var_x}$  (Difference in distribution only across x-axis)
  - $D_{var_{all}}$  (Difference in distribution in both facets and x-axis)



### 2.6.1 Environment

R version 4.0.1 (2020-06-06) is used with platform: x86\_64-apple-darwin17.0 (64-bit) running under: macOS Mojave 10.14.6 and MonaRCH, which is a next-generation HPC/HTC Cluster, designed from the ground up to address the computing needs of the Monash HPC community. The nodes and the storage used are as follows:

### 2.6.2 Results

This section reports the results of a simulation study that was carried out to evaluate the behavior of our distance measure across all potential factors. The results are reported in two parts: for the a) raw measure and then b) normalised one to show how the loopholes for the raw measures were removed using the normalized ones.

First, the behavior of  $wpd_{raw}$  and  $wpd_{norm}$  is explored in designs where there is no difference in distribution between  $x$  and facet categories. We have considered different initial distributions to study the impact of initial distribution under the null setup. Using two types of distributions, viz. normal and gamma (non-normal), we generated observations for each combination of  $nx$  and  $nfacet$  from the following sets:  $nx = \{2, 3, 5, 7, 14, 20, 31, 50\}$  and  $nfacet = \{2, 3, 5, 7, 14, 20, 31, 50\}$  to cover a wide range of levels from very low to moderately high. Each combination is being referred to as a *panel*. That is, data is being generated for each of the panels  $\{nx = 2, nfacet = 2\}, \{nx = 2, nfacet = 3\}, \{nx = 2, nfacet = 5\}, \dots, \{nx = 50, nfacet = 31\}, \{nx = 50, nfacet = 50\}$ . For each of the 64 panels,  $ntimes = 500$  observations are drawn for each combination of the categories. That is, if we consider the panel  $\{nx = 2, nfacet = 2\}$ , 500 observations are generated for each of the combination of categories from the panel, namely,  $\{(1, 1), (1, 2), (2, 1), (2, 2)\}$ . The values of  $\lambda$  is set to 0.67, since we want to up-weight the within-facet distances and that of  $\omega$  is set to 0, since there is no significant differences between distributions in the null case. Observations were generated for each type of distribution changing the shape and scale to study the effect of shape, scale and type of distribution on  $wpd$ . The set of distributions considered for this purpose is  $N(0, 1), N(5, 1), N(0, 5), \Gamma(0.5, 1), \Gamma(2, 1)$ . Each of the scenario is run  $nsim = 200$  times to see the distribution of  $wpd$  values for each scenario.

Secondly, the behavior of raw and normalized  $wpd$  is explored in designs where there is in fact difference in distribution between facet categories ( $D_{var_f}$ ) or across  $x$ -categories ( $D_{var_x}$ ) or both ( $D_{var_{all}}$ ). Using  $\omega = \{1, 2, \dots, 10\}$  and  $\lambda = seq(from = 0.1, to = 0.9, by = 0.05)$ , observations are drawn from a  $N(0, 1)$  distribution for each combination of  $nx$  and  $nfacet$  from the following sets:  $nx = nfacet = \{2, 3, 5, 7, 14, 20, 31, 50\}$ .  $ntimes = 500$  is assumed for this setup as well. Furthermore, to generate different distributions across different combination of facet and  $x$  levels, the following method is deployed - suppose the distribution of the combination of first levels of  $x$  and facet category is  $N(\mu, \sigma)$  and  $\mu_{jk}$  denotes the mean of the combination ( $a_j b_k$ ), then  $\mu_j = \mu + j\omega$  (for design  $D_{var_x}$ ) and  $\mu_k = \mu + k\omega$  (for design  $D_{var_f}$ ).

The tabulated values and graphical representations of the simulation results are provided in Appendix. The learning from the simulations are as follows: The values of the measure  $wpd_{raw}$  is least for  $D_{null}$ , followed by  $D_{var_f}$ ,  $D_{var_x}$  and  $D_{var_{all}}$ . This is a desirable result since the measure  $wpd_{raw}$  was designed such that this relationship holds. Furthermore, the distribution of the measure  $wpd_{raw}$  changes for different facet and  $x$  categories. The location of the distribution shifts to the right and it also becomes more skewed for more higher facet and  $x$ -axis categories. Now this is not desirable, as it would mean that we can't compare the  $wpd_{raw}$  values across different panels. The distribution of  $wpd_{norm}$  looks more similar with at least the mean and standard of the distributions being uniform across panels. This means,  $wpd_{norm}$  could be used to measure differences in distribution across panels. Also, note that since the data is processed using normal-quantile-transform, this measure is independent of the initial distribution of the underlying data and hence is also comparable across different datasets. This is valid for the case when sample size  $ntimes$  for each combination of categories is at least 30 and  $nperm$  used for computing  $wpd_{norm}$  is at least 100. More detailed results about the properties of  $wpd_{raw}$  and  $wpd_{norm}$  could be found in Appendix.

## 2.7 Properties

## 3 Choosing harmonies with significant wpd

## 4 Applications

### 4.1 Smart meter data of Australia

Smart meters provide large quantities of measurements on energy usage for households across Australia. One of the customer trials (Department of the Environment and Energy 2018) conducted as part of the Smart Grid Smart City project in Newcastle, New South Wales and some parts of Sydney provides customer wise data on energy consumption for every half hour from February 2012 to March 2014. The idea here is to show how to visualize the distribution of the energy consumption across different cyclic granularities in a systematic way to identify different behavioral patterns.

#### 4.1.1 50 households together

#### 4.1.2 Multidimensional scaling

#### 4.1.3 Putting similar households on linear scale

### 4.2 T20 cricket data of Indian Premiere League

The method is not only restricted to temporal data, and can be generalized to many hierarchical granularities (with continuous and uni-directional nature). We illustrate this with an application to the sport cricket. Although there is no conventional time component in cricket, each ball can be thought to represent an ordering from past to future with the game progressing forward with each ball. In the Twenty20 format, an over will consist of 6 balls (with some exceptions), an inning is restricted to a maximum of 20 overs, a match will consist of 2 innings and a season consists of several matches. Thus, similar to time, there is a hierarchy where ball is nested within overs, overs nested within innings and innings within matches. The idea of cyclic granularities can be likewise mapped to this hierarchy. Example granularities then include ball of the over, over of the inning and ball of the inning. Although most of these cyclic granularities are circular in design of the hierarchy, in application of the rules some granularities are aperiodic. For example, in most cases an over will consist of 6 balls with some exceptions like wide balls or when an inning finishes before the over finishes. Thus, the cyclic granularity ball-of-over will be circular in most cases and aperiodic in others.

The Indian Premier League (IPL) is a professional Twenty20 cricket league in India contested by eight teams representing eight different cities in India. The ball by ball data for IPL season 2008 to 2016 is fetched from Kaggle. The `cricket` data set in the `gravitas` package summarizes the ball-by-ball data across overs and contains information for a sample of 214 matches spanning 9 seasons (2008 to 2016) such that each over has 6 balls, each inning has 20 overs and each match has 2 innings. This could be useful in a periodic world when we wish to compute any circular/quasi-circular granularity based on a hierarchy table which look like Table 1.

However, even if the situation is not periodic and a similar hierarchy can not be formed, it can be interesting to visualize the distribution of a measured variable across relevant cyclic granularities to shed light on the aperiodic behavior of a non-temporal data set similar to aperiodic events like formal meetings, workshops, conferences, school semesters in a temporal set up. There are many interesting questions that could possibly be answered with such a data set irrespective of the type of cyclic granularities.

First, it would be interesting to see if the distribution of total runs vary depending on if a team bats in the first or second innings. The Mumbai Indians (MI) and Chennai Super kings (CSK) appeared in final playoffs from 2010 to 2015. We take their example in order to dive deeper into this question. From Figure

Table 1: Hierarchy table for cricket where overs are nested within an inning, innings nested within a match and matches within a season.

linear (G)	single-order-up cyclic (C)	period length/conversion operator (K)
over	over-of-inning	20
inning	inning-of-match	2
match	match-of-season	k(match, season)
season	1	1

6(a), it can be observed that for the team batting in the first inning there is an upward trend of runs per over, while there is no clear upward trend in median and quartile deviation of runs for the teams batting in the second inning. This seem to indicate that players feel mounting pressure to score more runs as they approach towards the end of the first inning. Whereas teams batting in the second inning have a set target in mind and are not subjected to such mounting pressure and may adopt a more conservative strategy, to score runs. Thus winning teams like CSK and MI seem to employ different inning strategies when it comes to their batting order.

Another interesting question could be: do runs per over decrease in the subsequent over if fielding (defending) was good in the previous over? For establishing the fielding quality, we apply an indicator function on dismissals (1 if there was at least one wicket in the previous over due to run out or catch, 0 otherwise). Runs in the current over is then the observation variable. Dismissals in the previous over can lead to a batsman adopting a more defensive play style. Figure 6(b) shows that no dismissals in the previous over leads to a higher median and quartile spread of runs per over as compared to the case when there has been at least one dismissal in the previous over.

Wickets per over are considered as an aperiodic cyclic granularity with wickets as an aperiodic linear granularity. These granularities do not appear in the hierarchy table since it is difficult to position them in a hierarchy. These are similar to holidays or special events in temporal data.

## 5 Discussion points and future work

Exploratory data analysis involve many iterations of finding and summarizing patterns. With temporal data available at ever finer scales, exploring periodicity has become overwhelming with so many possible granularities to explore. This work refines the selection of appropriate pairs of granularities by identifying those for which the differences between the displayed distributions is greatest, and rating these selected harmony pairs in order of importance for exploration.

A future direction of work could be to look at more individuals/subjects and group them according to similar periodic behavior. Behaviors across different cyclic granularities would be different for different subjects and one way to find groups would be to actually locate clusters who have similar periodic behavior.

## 6 Appendix

### 6.1 Null distribution

**6.1.1 Size: Simulated same distribution for all combinations of categories for all harmony pairs.**

Failure to reject the null hypothesis when there is in fact no significant effect.

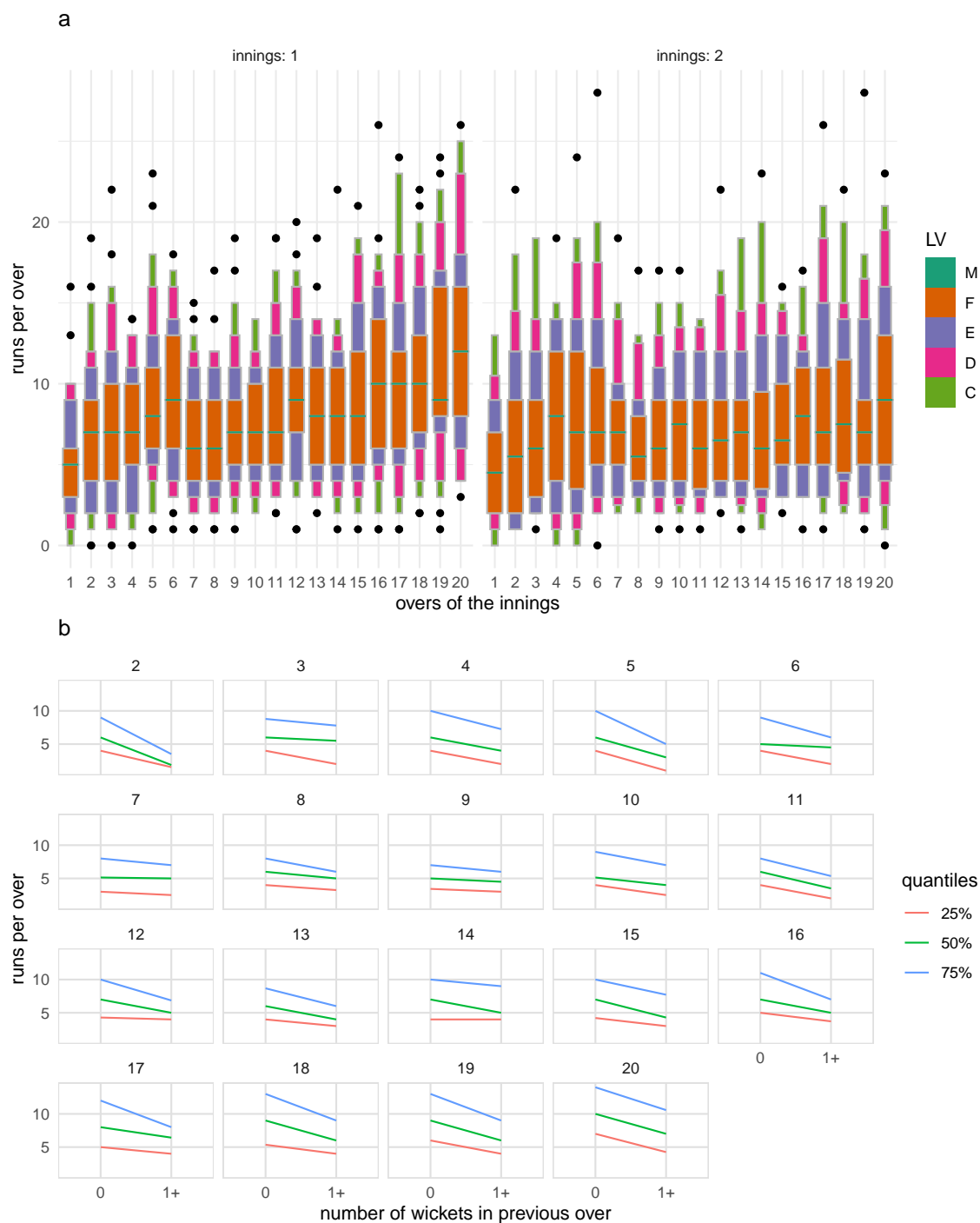


Figure 6: Runs per over shown with different distribution displays, and granularities. Plot (a) shows letter value plot across overs faceted by innings. For the team batting in the first innings there is an upward trend of runs per over, while there is no such pattern of runs for the teams batting in the second innings. Plot (b) shows quantile plot of runs per over across an indicator of wickets in previous over faceted by current over. This indicates that at least one wicket in the previous over leads to lower median run rate and quantile spread in the subsequent over.

### 6.1.2 Normalised maximum distances follow standard Gumbel distribution

### 6.1.3 Limiting distribution of median of normalised maximum distances is normal

Let a continuous population be given with cdf  $F(x)$  (cumulative distribution function) and median  $\xi$  (assumed to exist uniquely). For a sample of size  $2n + 1$ , let  $\tilde{x}$  denote the sample median. The distribution of  $\tilde{x}$ , under certain conditions, to be asymptotically normal with mean  $\xi$  and variance  $\sigma_n^2 = \frac{1}{4}[f(\xi)]^2(2n + 1)$ , where  $f(x) = F'(x)$  is the pdf (probability density function).

## 6.2 Power

## 6.3 Confidence interval

Failure to reject the null hypothesis when there is in fact a significant effect.

To estimate the sampling distribution of the test statistic we need many samples generated under the null hypothesis. If the null hypothesis is true, changing the exposure would have no effect on the outcome. By randomly shuffling the exposures we can make up as many data sets as we like. If the null hypothesis is true the shuffled data sets should look like the real data, otherwise they should look different from the real data. The ranking of the real test statistic among the shuffled test statistics gives a p-value.

### 6.3.1 Varying distribution across facet

### 6.3.2 Varying distribution across x-axis

### 6.3.3 Varying distribution across both facets and x-axis

### 6.3.4 Repeat all with varying facet and x-axis levels

*Conclusion:* The test should reject the null hypothesis if distributions are different.

Dang, T N, and L Wilkinson. 2014. “ScagExplorer: Exploring Scatterplots by Their Scagnostics.” In *2014 IEEE Pacific Visualization Symposium*, 73–80.

Department of the Environment and Energy. 2018. *Smart-Grid Smart-City Customer Trial Data*. Australian Government, Department of the Environment; Energy: Department of the Environment; Energy, Australia. <https://data.gov.au/dataset/4e21dea3-9b87-4610-94c7-15a8a77907ef>.

Gupta, Sayani, Rob J Hyndman, Dianne Cook, and Antony Unwin. 2020. “Visualizing Probability Distributions Across Bivariate Cyclic Temporal Granularities,” October. <http://arxiv.org/abs/2010.00794>.

Kullback, S, and R A Leibler. 1951. “On Information and Sufficiency.” *Ann. Math. Stat.* 22 (1): 79–86.

Menéndez, M L, J A Pardo, L Pardo, and M C Pardo. 1997. “The Jensen-Shannon Divergence.” *J. Franklin Inst.* 334 (2): 307–18.

Tukey, John W, and Paul A Tukey. 1988. “Computer Graphics and Exploratory Data Analysis: An Introduction.” *The Collected Works of John W. Tukey: Graphics: 1965-1985* 5: 419.

Wang, Earo, Dianne Cook, and Rob J Hyndman. 2020. “Calendar-Based Graphics for Visualizing People’s Daily Schedules.” *Journal of Computational and Graphical Statistics*. <https://doi.org/10.1080/10618600.2020.1715226>.

Wilkinson, Leland, Anushka Anand, and Robert Grossman. 2005. “Graph-Theoretic Scagnostics.” In *IEEE Symposium on Information Visualization, 2005. INFOVIS 2005.*, 157–64. IEEE.